J. Biochem. 126, 226-234 (1999)

Binding of Cholera Toxin B-Subunits to Derivatives of the Natural Ganglioside Receptor, GM1

Boel Lanne,*[,1] Birgitta Schierbeck,[†] and Jonas Ångström*

*Institute of Medical Biochemistry, Göteborg University, P.O. Box 440, SE 405 30 Göteborg, Sweden; and †College of Health and Caring Sciences, Department of Medical Laboratory Science, Göteborg University, Box 419, SE 405 30 Göteborg, Sweden

Received March 18, 1999; accepted May 10, 1999

In a previous paper we showed that the B-pentamer of cholera toxin (CT-B) binds with reduced binding strength to different C(1) derivatives of *N*-acetylneuraminic acid (NeuAc) of the natural receptor ganglioside, GM1. We have now extended these results to encompass two large amide derivatives, butylamide and cyclohexylmethylamide, using an assay in which the glycosphingolipids are adsorbed on hydrophobic PVDF membranes. The latter derivative showed an affinity approximately equal to that earlier found for benzylamide (~0.01 relative to native GM1) whereas the former revealed a approximately tenfold further reduction in affinity. Another derivative with a charged C(1)-amide group, aminopropylamide, was not bound by the toxin. Toxin binding to C(7) derivatives was reduced by about 50% compared with the native ganglioside. Molecular modeling of C(1) and C(7) derivatives in complex with CT-B gave a structural rationale for the observed differences in the relative affinities of the various derivatives. Loss of or altered hydrogen bond interactions involving the water molecules bridging the sialic acid to the protein was found to be the major cause for the observed drop in CT-B affinity in the smaller derivatives, while in the bulkier derivatives, hydrophobic interactions with the protein were found to partly compensate for these losses.

Key words: amide and amine derivatives, cholera toxin, GM1 receptor binding, molecular modeling, sialic acid chemical modification.

The bacterium *Vibrio cholerae* produces a toxin (CT) that causes severe diarrhea in humans. This heterohexameric protein consists of a catalytic A-subunit anchored in the central pore of a B-pentamer responsible for binding to cell surface-located receptor molecules. Although the specific target cells in the intestinal epithelium to which the released toxin binds are not fully known, it is generally assumed that the receptor is the acidic glycosphingolipid GM1, Galβ3GalNAcβ4(NeuAcα3)Galβ4Glcβ1Cer (*1*). After internalization and cleavage of the A-subunit into A1 and A2, the former fragment adenylates an Arg in the regulatory G-protein, which in turn irreversibly activates adenylate cyclase (review, *2*). It is also assumed that the nervous system in the intestine is involved since this system is activated by the toxin (review, *3*) and because nerve cells in general are rich in GM1 (*4*).

One way of assessing the contributions of individual interactions in the binding of carbohydrate by protein is to perform small and specific chemical modifications of the epitopes being recognized (*5, 6*). Several papers have thus been published reporting results of CT-B binding to natural or synthetic analogues of GM1 (*7-13*). In conjunction with studies of the three-dimensional structure of glycosphingolipids using molecular modeling, further information on the binding epitopes may be obtained (*7, 14*). Ideally such studies should entail the use of proteins for which the atomic structures are known, which is the case for CT-B (*15, 16*), enabling a deeper understanding of binding at the molecular level.

When the binding strength of lectins or antibodies to glycoconjugates are measured, the latter are often adsorbed in microtiter wells. However, such analyses are often performed over a rather narrow range of carbohydrate concentration due to nonlinearity (*12, 17*). In the present paper an alternative approach was employed to compare the CT-B affinity of different ligands using serially diluted glycosphingolipids adsorbed onto hydrophobic membranes. This method was found to yield a linear response over a considerably broader ligand concentration range, allowing more accurate determinations of relative binding strengths. Molecular modeling of different C(1)-amide and C(7)-amine sialyl derivatives of GM1 in complex with

[1] To whom correspondence should be addressed: Astra Hässle AB, S-431 83 Mölndal, Sweden. Tel: +46-31-776-2864, Fax: +46-31-776-3736, E-mail: boel.lanne@hassle.se.astra.com

Abbreviations: CT-B and LT-B, B-subunits of cholera toxin and the heat-labile toxin from porcine *E. coli*, respectively, in pentameric form; d20:1-18:0; a ceramide composed of sphingosine with 20 carbon atoms and a saturated fatty acyl chain with 18 carbon atoms. The number of unsaturated bonds is indicated by the digit after the colon. EI MS, electron impact mass spectrometry; FAB, fast-atom bombardment; GM1, Galβ3GalNAcβ4-(NeuAcα3)Galβ4Glcβ1Cer; GM2, GalNAcβ4(NeuAcα3)Galβ4Glcβ1Cer; MS, mass spectrometry; PVDF, polyvinylene difluoride; TLC, thin-layer chromatography.

CT-B have provided additional insight into the subtle molecular mechanisms underlying the affinity changes observed here.

MATERIALS AND METHODS

Chemicals—The gangliosides GM1 and GM2 were purified from human brain (*4, 18*). The purity of the isolated gangliosides was confirmed by TLC and negative-ion FAB MS and positive-ion EI MS after methylation and methylation-reduction-methylation (*19, 20*). The ceramide of GM1, used for derivatizations, was composed mainly of d18:1-18:0 and d20:1-18:0 (approx. 4:5) and GM2 of d20:1-18:0, d20:1-16:0, and d20:1-20:0 (approx. 5:4:1). CT-B was purchased from Sigma Chem., MO, USA, or from LIST Biological Laboratories, CA, USA, and labeled with ^{125}I (*21*) in 0.1 M sodium phosphate buffer, pH 7.2. CT-B conjugated with horse radish peroxidase (HRP) was purchased from Sigma Chem. and diaminobenzidine from DAKO, Denmark. Cyclohexylmethylamine ($NH_2CH_2C_6H_{11}$) (98%), 1,3-diaminopropane ($NH_2(CH_2)_3NH_2$) (90%), 2-aminobutane ($CH_3NH_2CHCH_2CH_3$), 1-aminobutane ($NH_2(CH_2)_3CH_3$), glycine (NH_2CH_2COOH), and methyl iodide were purchased from Aldrich, Germany, DEAE-Sepharose CL-6B and Q Sepharose Fast Flow from Pharmacia, Sweden, thin-layer plates (HPTLC), both glass- and aluminum-backed, from Merck, Germany, and the HPLC column, Spherisorb S10W silica column, 250×8 mm inner diameter, particle size 10 μm from Phase Separation, UK.

Glycosphingolipid Derivatizations and Characterization—Derivatizations of GM1 to different sialyl C(1)-amides as well as the purification procedures have been described (*10*). To test the stability of these derivatives, two-dimensional TLC was performed as previously described (*22*). Derivatization of GM1 to different C(7)-amines of NeuAc started with periodate oxidation according to Ref. *23*, by dissolving 0.5 mg/ml of GM1 in 0.1 M $NaCH_3COO$, pH 5.5, 0.15 M NaCl, 0.013 M $NaIO_4$. The reaction was allowed to proceed for 15 min at 0°C in the dark. The reaction was stopped by the addition of glycerol. One volume of methanol was added and the solution was applied to a SepPac disposable column (C18, 100 mg, Altech, IL, USA) (*24*) in order to separate the aldehyde from GM1. The column was washed with 30 ml of deionized water, then the derivatives were eluted with 10 ml of methanol and lyophilized. The aldehyde was dissolved in methanol (0.5 mg/ml) and a surplus of amine reagent (1,000:1) and approx. 2 mg of $NaBCNH_3$ were added. Another addition of $NaBCNH_3$ was made after 30 min, and 1 h later approx. 4 mg of $NaBH_4$ was added. After a total of 2 h, 2 ml of water was added and the sample was lyophilized. After this, the mixture was dissolved in 200 μl water/methanol, 1:1 (by vol unless otherwise stated), and desalted on a reversed phase, C18, SepPac column, 100 mg, as described above. The solvent was evaporated with a stream of N_2(g).

HPLC purification of approx. 4 mg of each derivative was performed on a silica column with chloroform/methanol/water as the eluent (2 ml/min); the butylamide, cyclohexylmethylamide, methylamine, and benzylamine derivatives were eluted with a gradient from 65:25:4 to 50:40:10, and the carboxymethylamine derivative with a gradient from 60:35:8 to 50:40:10. The methylamine and benzylamine derivatives were further purified by ion-exchange chromatography on Sepharose Q. The samples were dissolved in approx. 1 ml of chloroform/methanol, 2:1, and applied to a column, 150 mm×10 mm inner diameter, equilibrated in chloroform/methanol, 2:1. The methylamine derivative was eluted with methanol and found to elute after GM1. For the benzylamine derivative, GM1 was first eluted with methanol and thereafter the derivative was eluted with 0.04 M NH_4HCO_3 in methanol. The purities of the derivatives were tested by TLC.

Quantitative determination of native and derivatized glycosphingolipids was made by determination of hexose (*25*) and detection of sugar on TLC plates with anisaldehyde or resorcinol spraying (*26*).

Mass spectra were recorded with a Jeol SX-102 (JEOL, Japan) sector instrument operating either in the positive-ion EI mode or in the negative-ion FAB mode with Xe-atom bombardment (6 keV) using triethanolamine as the matrix and an accelerating voltage of 10 keV.

Binding Assays—Incubation of toxin with glycolipids in microtiter wells and on thin-layer plates (*27*) was performed in the presence of 30 nM ^{125}I-labeled CT-B (expressed as subunit B monomers) in PBS (8 mM phosphate buffer, pH 7.3, 0.15 M NaCl, 4 mM KCl) and 2% BSA. Incubation times were always 2 h. Unless otherwise stated, all TLC separations were made with chloroform/methanol/water, 60:35:8. To estimate the binding of CT-B to glycolipids on PVDF blotting membranes (Immobilon P, Millipore, MA, US), 4 μl of each test solution was applied to the same membrane (100 mm×100 mm). The membrane was treated exactly as the TLC plates, except that treatment with plastic solution (polyisobutylmethacrylate) was not done.

Radioactivity on TLC plates was detected by autoradiography (Kodak XAR-5 film, Eastman Kodak, NY, US), and radioactivity in the wells was measured with a γ-counter (LKB, 1282 Compugamma). Binding to PVDF membranes was measured in either of two ways: with an excitable phosphorescent screen analyzed with a BioRad GS-250 Molecular Imager (BioRad Laboratories, CA, US) or with a γ-counter after excizing each glycolipid spot. The binding spots were quantitated with Phosphor Analyst™ (BioRad) software. This gave a linear response over at least three orders of magnitude. HPR-conjugated CT-B was used in the same way as the iodine-treated B-pentamer and incubated with the TLC-separated glycolipids, visualized with diaminobenzidine as described in Ref. *28* with intensity enhancement as described in Ref. *29*.

Molecular Modeling—GM1 and the various derivatives were constructed with the Biograf software package from Molecular Simulations (Waltham, MA, USA) on a Silicon Graphics 4D/35TG workstation using the Dreiding-II force field (*30*). Charges were generated by the charge equilibration method (*31*); a distance-dependent dielectric constant ($\varepsilon = 3.5r$) was used in energy minimizations in which a hydrogen bonding term was added (*30*). Starting values for the glycosidic dihedral angles of GM1 were taken from the CT-B complex (*15*) except for the Galβ4Glc angles (*32*). Favored conformations of the modified carboxyl groups of some of the derivatives were investigated by rotating the O5-C2-C1-O dihedral angle in 5° steps applying 100 steps of conjugate gradient energy minimization for each increment. Each derivative was tested two times with different orientations of the 8-OH of the glycerol tail since this group

significantly affects the outcome of the conformational search. The structures were subsequently minimized further at the found minima.

For docking of the different GM1 derivatives to CT-B (PDB entry 1CHB) and the ensuing dynamic runs, the structures were transferred to the Quanta97/CHARMm22 software package on a Silicon Graphics Indigo²Extreme workstation. In order to reduce the computational time a region of two B subunits consisting of 40 amino acids (H: 1-16, 51-69, 88-91; D: 31-36) surrounding one of the GM1 binding sites was selected from the crystal structure (*15*) and allowed freedom of movement. Previously energy minimized GM1 derivatives were docked into the binding site by overlapping all sugar units as closely as possible with the corresponding sugars in the crystal structure. Subsequently the ligand was further energy minimized while keeping the protein fixed. As a last step the whole complex was minimized without constraints using a distance-dependent dielectric constant ($\varepsilon = 6r$). Some of the complexes thus produced were subjected to molecular dynamics simulations (100 ps) after initial heating (6 ps using 5 K increments up to 300 K) and equilibration (10 ps) periods. All bonds to hydrogen were constrained by the SHAKE algorithm allowing a time step of 2 fs.

RESULTS AND DISCUSSION

CT-B Binding and Structural Characterization of GM1 Derivatives—Preliminary binding tests of CT-B to a series of unpurified C(1)-amide derivatives of GM1, cyclohexylmethylamide, methylpropylamide, butylamide, and aminopropylamide, are shown in Fig. 1A. Small amounts of native GM1 remain in all samples and give binding. Strong binding is also obtained at the R_f of the GM1 lactone for samples with methylpropylamide and carboxymethylamide (the latter not shown), and more weakly to the sample with cyclohexylmethylamide. This result is in accordance with FAB MS showing mainly the lactone of GM1 (loss of 18 amu from native GM1) for the methylpropylamide and carboxymethylamide samples. The derivatization to C(1)-aminopropylamide was almost quantitative, but CT-B did not bind to this derivative (Fig. 1A). CT-B bound, however, to cyclohexylmethylamide- and butylamide-GM1 and these derivatives were therefore purified by ion-exchange chromatography. In Fig. 1B, the binding of CT-B to the purified cyclohexylmethylamide and butylamide derivatives of GM1 is shown together with the binding to the previously reported benzylamide derivative and GM1 as a reference. Chemical staining of these purified amides is shown in Fig. 1C. The C(7)-amines of GM1 sialic acid were prepared as described in "MATERIALS AND METHODS" and purified by straight phase HPLC followed by ion-exchange chromatography. After purification, TLC analyses with either chemical staining or CT-B binding (Fig. 1D) showed the absence of unmodified GM1.

The FAB mass spectra of six GM1 derivatives are shown in Fig. 2, whereas theoretical weights and fragmentations are shown in Table I and Fig. 3, respectively. For the C(1)-amide derivatives butylamide and cyclohexylmethylamide, intense $[M-H]^{-1}$ ions were obtained corresponding to the two sets of ceramides present. Loss of the modified sialic acid also gives prominent ions at m/z, 1,281.8 and 1,253.8, and fragmentations at the other glycosidic bonds are apparent. The aminopropylamide derivative was not purified prior to the MS analysis and the fragmentation differed slightly from the other amides. The $[M-H]^{-1}$ ions appear rather weak, while loss of the derivatized sialic acid gives stronger ions. Except for the loss of the terminal Gal all other expected fragmentation ions are seen in the spectrum. The mass spectra of three C(7)-amine derivatives of GM1 are shown in Fig. 2, D-F. For both methylamine and benzylamine $[M-H]^{-1}$, all possible ions from cleavage at the glycosidic bonds were present, *cf.* Table I. For the carboxymethylamine derivative of GM1, however, peaks originating from the loss of the terminal Gal and the penultimate GalNAc were rather weak while $[M-H]^{-1}$ was strong as were fragments originating from the loss of the modified sialic acid.

Based on the MS data and binding tests of CT-B on TLC plates, the following GM1 derivatives were further evaluated with regard to their binding strength relative to the native receptor: C(1)-butylamide, C(1)-cyclohexylmethylamide, C(7)-methylamine, C(7)-benzylamine, or C(7)-carboxymethylamine. In some tests the C(1)-methylamide, C(1)-benzylamide, and C(1)-alcohol derivatives were included as references (*10*).

A comparison of the two methods used for assaying the binding of iodinated CT-B to native GM1 is shown in Fig. 4A. In both cases, serial dilutions of the glycolipids were adsorbed on a solid support, either in conventional microtiter wells or on PVDF membranes, before incubation with toxin solution. The results show that the amount of radioactivity obtained in the microtiter wells reached a maximum at around 10 pmol GM1 per well and then decreased

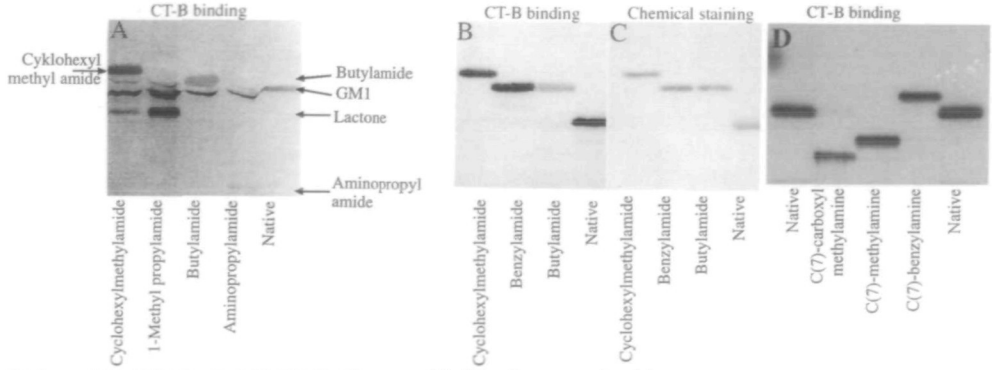

Fig. 1. **TLC analysis of GM1 derivatives visualized by the binding of ^{125}I-labeled CT-B.** In (A) a series of unpurified C(1)-amides are shown; in (B) three of these amide derivatives are shown after purification. Anis aldehyde staining of these purified derivatives is shown in (C). (D) shows CT-B binding to purified C(7)-amine derivatives. Native GM1 is included as a reference in all chromatograms. The chromatographic eluent in (A) was chloroform / methanol / water 60:45:10, in (B) and (C) 60:35:8, and in (D) 60:40:9 (0.2% $CaCl_2$ was added to the water in this case).

on further addition of GM1. When increasing amounts of GM1 were immobilized on PVDF membranes, on the other hand, the amount of bound CT-B continued to increase up to at least 100 pmol GM1/spot. The observed decrease in

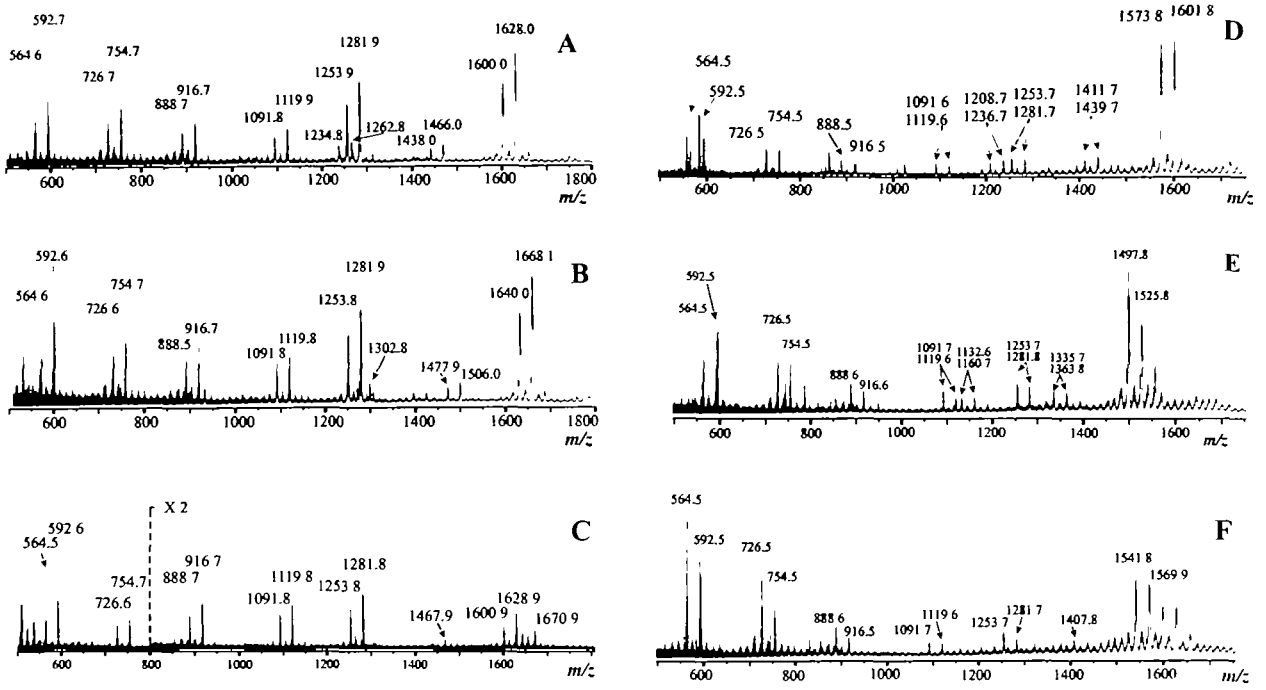

Fig. 2. **Negative-Ion FAB mass spectra of GM1 derivatives.** (A) C(1)-butylamide, (B) C(1)-cyclohexylmethylamide, (C) C(1)-aminopropylamide, (D) C(7)-benzylamine, (E) C(7)-methylamine, and (F) C(7)-carboxymethylamine. The C(1)-aminopropylamide of GM1 was not purified before MS analysis. Theoretical fragmentations are shown in Table I.

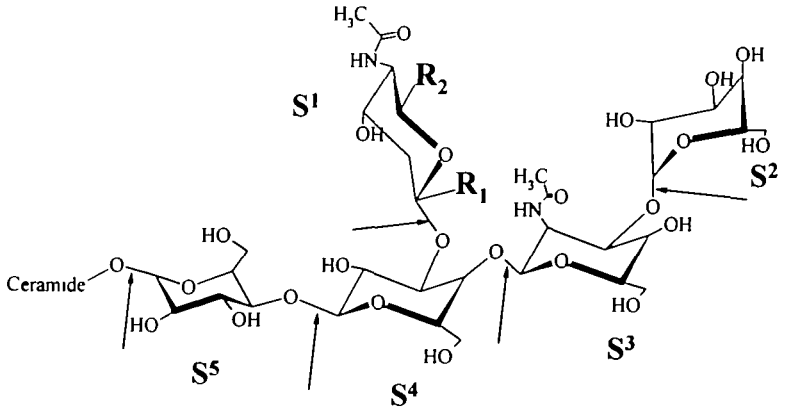

Fig. 3. **Structure of GM1 derivatives and FAB-MS fragmentations.** See Table I for substituents (R) and weight of fragments.

TABLE I. **Theoretical FAB-MS fragmentations of GM1 derivatives.**

Compound[a]	M-1	M-S²	M-(S²+S³)	M-S¹	M-(S¹+S²)	S⁴S⁵Cer	S⁵Cer	Cer
A R_1=CONH(CH_2)$_3CH_3$	1,599.9	1,437.9	1,234.8					
C(1)-butylamide	1,627.9	1,465.9	1,262.8					
B R_1=CONH$CH_2C_6H_{11}$	1,640.0	1,477.9	1,274.9					
C(1)-cyclohexylmethylamide	1,668.0	1,505.9	1,302.9					
C R_1=CONH(CH_2)$_3NH_2$	1,600.9	1,438.9	1,235.8	1,253.8	1,091.7	888.7	726.6	564.5
C(1)-aminopropylamide	1,628.9	1,466.9	1,263.8	1,281.8	1,119.7	916.7	754.6	592.6
D R_2=CH_2NH$CH_2C_6H_5$	1,573.9	1,411.9	1,208.8					
C(7)-benzylamine	1,601.9	1,439.9	1,236.8					
E R_2=CH_2NHCH_3	1,497.9	1,335.9	1,132.8					
C(7)-methylamine	1,525.9	1,363.9	1,160.8					
F R_2=CH_2NHCH_2COOH	1,541.9	1,379.8	1,176.8					
C(7)-carboxymethylamine	1,569.9	1,407.9	1,204.8					

[a]Weights are shown for two sets of ceramides: d18:1-18:0 (upper) and d20:1-18:0 (lower).

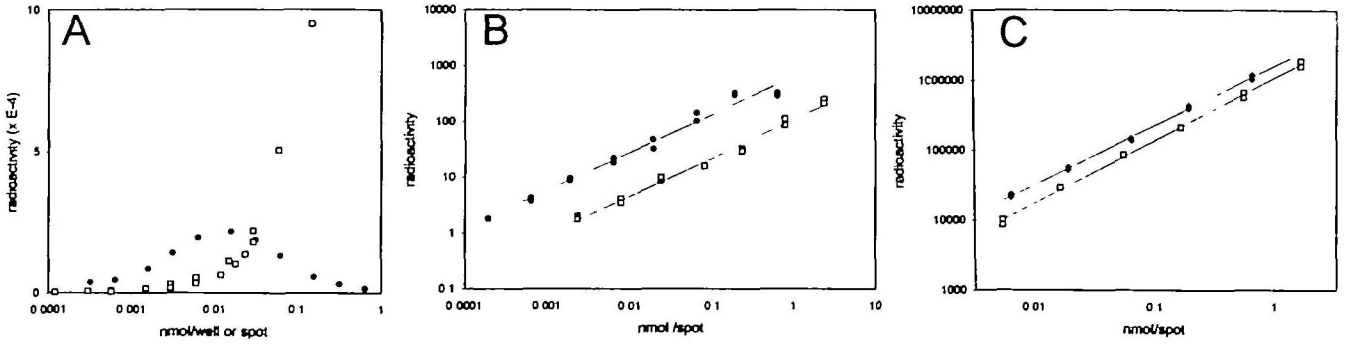

Fig. 4. **Binding of ^{125}I-labeled CT-B to native GM1 and to amide and amine derivatives.** In (A) a comparison is made between binding to serial dilutions of GM1 in microtiter wells (filled circles) and on a PVDF membrane (two separate experiments, open squares). The incubation media contained the same concentration of CT-B and the same number of washing steps were used after toxin incubation. (B) and (C) show comparisons of the binding to GM1 (filled symbols) and the C(1)-amide (B) and C(7)-benzylamine (C) derivatives (open symbols), on PVDF membranes.

TABLE II. **Relative binding affinity of CT-B for different GM1 derivatives.**

Glycolipid	Relative binding constant (K_{rel})[a]	$\Delta(\Delta G)$ (kcal/mol)[b]
GM1	1	0
GM2	0.015	2.5
C(1) derivatives		
alcohol	0.030	2.1
amide	0.073	1.5
butylamide	0.001	4.1
cyclohexylmethylamide	0.011	2.7
benzylamide	0.012	2.6
C(7) derivatives		
methylamine	0.41	0.5
benzylamine	0.56	0.3
carboxymethylamine	0.35	0.6

[a]Mean value of three separate determinations. [b]Calculated according to $\Delta(\Delta G) = -RT \ln (K_1/K_2) = -RT \ln (K_{rel})$.

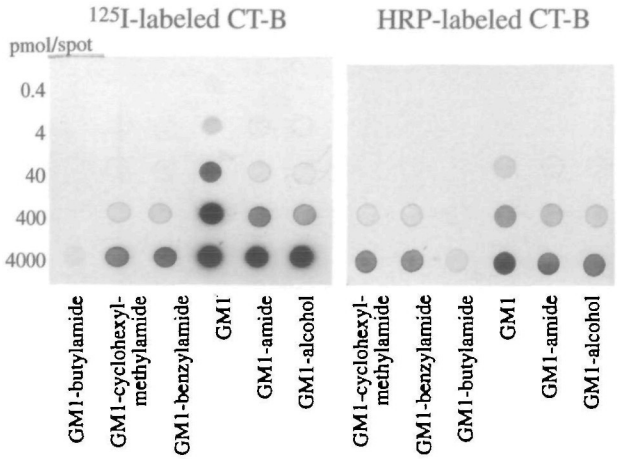

Fig. 5. **Binding of CT-B to GM1 and its derivatives on PVDF membranes.** CT-B was labeled with either ^{125}I or HRP. The glycolipids were applied in serial dilutions with 0.4, 4, 40, 400, or 4,000 pmol per spot.

binding in microtiter wells is not yet fully understood, but has been ascribed to peeling effects when the limit of one glycolipid monolayer is crossed, which may facilitate the formation of micellar structures that are subsequently lost in the washing procedure (*33*). It has also been shown that the more charges a glycolipid carries, the greater the problem of loss from the microtiter wells (*17, 34*). On PVDF membranes, however, the glycolipids are very firmly attached and are not even eluted during extensive washing procedures including water or water/ethanol treatment (*35*).

In most binding experiments CT-B was iodinated in order to allow monitoring of binding. To confirm that the iodination procedure did not disturb the binding specificity of the toxin, the bindings of HRP-conjugated and iodinated CT-B to some of the GM1 derivatives, applied on hydrophobic PVDF membranes, were compared (Fig. 5). As can be seen, the relative binding of any of the six compounds tested, native GM1 and five C(1)-amides, was very similar irrespective of the technique used for labeling.

As the method utilizing a hydrophobic membrane as a solid support for the binding of CT-B allowed measurement over larger ranges of ligand concentration, this method was chosen for further comparisons of the binding strengths of native GM1 and the C(1)- and C(7)-derivatives. The analyses were always performed so that the unmodified GM1 and a derivative were applied to the same PVDF membrane, and, therefore, binding relative to GM1 was always measured. Two examples are shown in Fig. 4, B and C, where CT-B binding to GM1 is compared to that of the C(1)-amide and C(7)-benzylamine derivatives, respectively. The amount of radioactivity of each spot with glycolipid on the PVDF membranes was measured with a Phosphor imager and plotted against the amount of ganglioside applied to each spot (log/log scale). This gave straight lines covering about 3 orders of magnitude. Saturation binding was not determined so that the absolute value for K_B could not be determined. However, assuming that one glycolipid is bound per B-subunit, the relative K_B values for the derivatives can be obtained. By comparing the amounts of each glycolipid required to give a certain amount of radioactivity (displacement along the x-axis) the relative binding strengths, K_{rel}, of the different derivatives and associated free energy changes were calculated (Table II). For comparative purposes, binding to GM2 was also included in the analyzes. As expected (*7, 8, 12*) this binding was weaker than the binding to GM1.

Structural Analysis by Molecular Modeling—Early

NMR and molecular modeling studies showed that the three-dimensional structure of the GM1 pentasaccharide is relatively rigid due to the sialic acid attached to the internal galactose (*36, 37*). The glycosidic dihedral angles of the sialic acid thus assume the *anticlinal* conformation ($\phi \approx -170°$, $\Psi \approx -30°$) that is stabilized by an inter-residue hydrogen bond between the sialic acid carboxyl group and the -NH of the GalNAc acetamido moiety (*38*) and a sialic acid intraresidue hydrogen bond between the 8-OH of the glycerol tail and the second carboxylate oxygen (*39*). This picture was subsequently confirmed by the appearance of the GM1-CT-B crystal structure (*40*). The GM1 C(1) derivatives have a common denominator in that the modified carboxyl group retains the ability to form hydrogen bonds with the GalNAc acetamido moiety and/or the 8-OH of the glycerol tail when oriented accordingly. However, as will be evident from below, the orientation of the chemically modified carboxyl function is critical for the ability of these derivatives to bind to CT-B. The Ω dihedral angle of the chemically modified sialic acid, defined as O5-C2-C1-O1, may thus for the hydroxyl derivative assume values corresponding to the three staggered positions at ±60° and 180°, whereas the different amide derivatives may only assume values close to −60° and 180°. The +60° orientation is disallowed due to steric interference with the acetamido moiety of the GalNAcβ4 residue. For smaller derivatives, the −60° conformer (∼−45° after energy minimization) is energetically somewhat favored over the 180° conformer, allowing maximal hydrogen bonding in each case by reorienting the 8-OH of the glycerol tail, whereas for bulkier substituents, interactions with the terminal Galβ3 residue make accurate estimates difficult. On the other hand, only one of these orientations is sterically allowed in the CT-B complexes of these latter derivatives (see below) including the methylamide derivative.

In the crystal structure of the native CT-B-GM1 complex one of the sialic acid carboxylate oxygens forms an important hydrogen bond with the backbone NH of His13 (Fig. 6) and, as mentioned above, the second oxygen forms an interresidue hydrogen bond with the acetamido group of GalNAcβ4. The complex is further stabilized by hydrogen bonds between the sialic acid and different amino acids *via* three bridging water molecules whereas a fourth water molecule involves the terminal galactose as shown in Fig. 6 (*15*). Docking the different GM1 derivatives into the binding site reveals that for the hydroxyl and amide derivatives either of the two orientations of the modified carboxyl function may be accommodated without steric interference from the protein, and that, furthermore, all four internal waters most likely are retained but with slightly altered orientations and/or positions. Despite the fact that the −60° orientation is favored for the free hydroxyl derivative, it is very likely that the conformation present in the complex in this case is the 180° one (164° after minimization) since this causes minimal disturbance of the hydrogen bond network involving the internal water molecules, resulting in loss of the bridging bond to the Trp88 indole NH and the bond between the inner carboxyl oxygen and the His13 backbone carbonyl oxygen bridged by water molecule 1 (Fig. 6). Importantly, the direct hydrogen bond to the His13 backbone NH is retained in this case. Consistent with this conclusion, it was found that the 180° conformation is favored by approximately 1.9 kcal/mol in the complex. In the alternative conformation, hydrogen bonds to both the His13 and Gly33 backbone NH groups are lost and unfavorable interactions between the C(1) methylene protons and the former group are found. For the complex of the amide derivative, the 180° conformation is favored by 3.6 kcal/mol over the −60° one, mainly due to the loss of a hydrogen bond to His13 in the latter conformation as well as unfavorable interactions between the amide -NH_2 and the His13 backbone NH. The loss of the indirect hydrogen bonds to the Gly33 NH (due to the amide -NH_2 group which also reorients the 8-OH) as well as to the Trp88 NH and His13 CO (analogous to the hydroxyl derivative) when the amide is in the 180° conformation is thus most likely the leading cause for the observed drop in the CT-B affinity for this derivative.

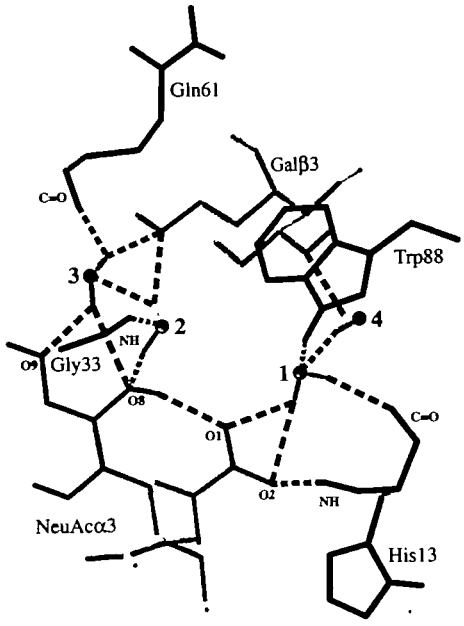

Fig. 6. **View of the GM1 binding site region in CT-B showing the structural role played by internal water molecules (labeled 1-4) in anchoring the sialic acid part of GM1 in the binding site [produced using the crystal structure obtained from (*15*)].** Only the terminal galactose and the sialic acid of GM1 (light gray) and amino acids (dark gray) participating in the hydrogen bond network involving the water molecules are shown.

It was found that the other C(1) derivatives may be accommodated within the binding site, by displacing one or more of the internal water molecules, only when the 180° conformation of the modified carboxyl group is present. Thus, for the methylamide derivative, which is only slightly binding-active (*10*), water molecule 1 (Fig. 6) is most likely displaced by the amide methyl group, resulting in the loss of the hydrogen bond interactions involving this water molecule. Enlarging the hydrophobic moiety on the substituted amide to an ethyl or propyl group would also gradually affect water molecules 2 and 3, thus rendering these derivatives inactive. However, for the larger butyl-, cyclohexylmethyl-, and benzylamide derivatives, hydrophobic interactions with surrounding amino acid side chains that compensate for the loss of the water-mediated interactions become apparent. This is exemplified by the complex

between the benzylamide derivative and CT-B shown in Fig. 7. The benzylamide moiety makes van der Waals contacts with the glycerol tail, the Tyr12, Trp88, Gly33, and Ile58 side chains, as well as with the Galβ3GalNAcβ4 segment of GM1. Conformational changes in this derivative are restricted to a change in the Φ dihedral angle of NeuAcα3Gal, from $-169°$ in the native complex to $-150°$ in the derivative, resulting in a slight tilt in the sialic acid ring plane induced by the benzylamide moiety, and a slight downward movement (as seen in Fig. 7) of the Galβ3GalNAcβ4 segment of approximately 0.5 Å. The hydrogen bond between the carbonyl oxygen of the benzylamide moiety and the backbone NH of His13 as well as that between the acetamido NH of the sialic acid and the backbone carbonyl oxygen of Glu11 are present as in the native complex. The stability of the complex was tested during a 100 ps dynamics run at 300 K in which all the interactions described above were found to be retained throughout the simulation period. In contrast, the same somewhat distorted complex with the benzylamide moiety in the $-60°$ conformation showed clear signs of dissociation of the derivative from the binding site towards the end of an equally long simulation. The CT-B complexes of the butyl- and cyclohexylmethylamide derivatives are very similar in behavior to the benzylamide derivative, both revealing a similar tilt of the sialic acid. Furthermore, for all three complexes, water molecules 1 and 4 may still be retained due to the slight reorientation of the modified sialic acid.

Finally, the effect of replacing the C(8)-C(9) segment of the sialic acid glycerol tail of GM1 with either methylamine, carboxymethylamine, or benzylamine reduces the binding strength by approximately 50% (Table II), which may be rationalized by examination of Figs. 6 and 8. Internal water molecules 2 and 3 will no longer be able to provide the stabilizing hydrogen bond interactions present in the native complex, but they are likely to remain since no steric interference can be discerned in either derivative. For the methylamine derivative the terminal methyl group is able to form a hydrophobic patch with the Ile58 side chain and probably also with the inner part of the Lys34 side chain, which partly compensates for the loss of these hydrogen bonds. The addition of a terminal carboxyl group does not interfere sterically with the protein since this moiety is pointing towards the surrounding medium while the hydrophobic interactions are somewhat lessened; the hydrophobic interactions in the benzylamine derivative, however, are slightly enhanced. For the carboxymethylamine derivative, Lys34 may also form a stabilizing salt bridge with the carboxyl group. These observations are corroborated by the relative free energy changes given in Table II as discussed below.

Correlation between Structural and Free Energy Changes—Molecular modeling of the complexes between CT-B and the different C(1) and C(7) sialyl derivatives of GM1 shows that the main structural changes result from the expulsion and/or reorientation of the internal water molecules involved in anchoring the sialyl residue to the protein surface, leading to the loss of hydrogen bond interactions in some cases or new hydrophobic interactions in other cases. Conformational changes in either the protein and/or ligand are very restricted and can only be ascertained with some confidence for the bulkier C(1) derivatives, but would at most have very modest energy contributions. Binding data from techniques that use glycosphingolipids in liposomes or as free oligosaccharides (*11, 41-45*) do not lend themselves to comparisons with the data obtained by the present assay for a variety of reasons. Different microenvironments affect the epitope presentation to varying degrees: conformational restrictions around *e.g.* the glucose-ceramide linkage are thus less evident in TLC, microtiter well, and PVDF membrane assays than in assays involving lipid bilayers, and even then lipid composition and receptor concentration play important roles in discriminating between different isoreceptors. Since the simpler assays provide conformationally less constrained environments, the use of a range of structurally related receptors may allow delineation of the binding epitope while more restricted environments may yield information

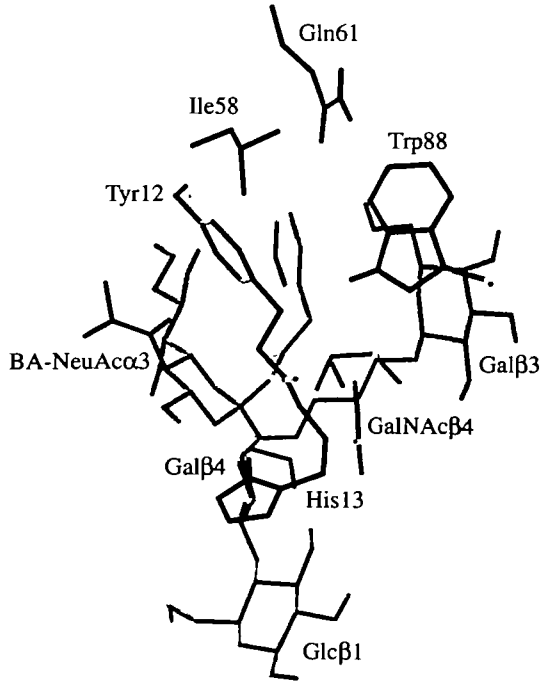

Fig. 7. **Model of the complex between the C(1)-benzylamide (BA) derivative of GM1 (light gray) and CT-B (dark gray) showing the benzylamide moiety inserted into the pocket occupied by internal water molecules in the native complex.**

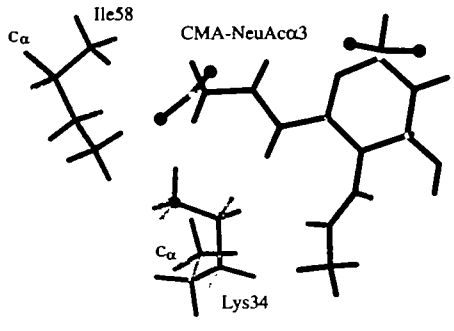

Fig. 8. **Model of the modified sialyl residue of the C(7)-carboxymethylamine (CMA) derivative of GM1 (dark gray) and the interactions of the carboxymethylamine substituent with the two closest CT-B residues (light gray).** Carboxyl oxygens are indicated as small spheres.

regarding *in vivo* specificities and functionality. It is, therefore, usually preferable to employ more than just a single assay depending on the properties that need to be evaluated. In the present case, as few restrictions as possible were desirable in order to pick up weak relative binding affinities that could be related to structural changes in the different complexes.

A qualitative assessment, in terms of energetic cost, of the structural changes induced by the introduction of different substituents on the sialic acid can be made, nevertheless, and correlated with the calculated free energy changes given in Table II. Loss of hydrogen bonds involving neutral donor-acceptor pairs have been found to reduce affinity by 0.5-1.5 kcal/mol whereas the loss of hydrogen bonds involving a charged donor (acceptor) result in a reduction of 3.5-4.5 kcal/mol as observed for the site-directed mutagenesis of the active site of tyrosyl-tRNA synthase (*46*). Replacement of a charged donor (acceptor) with a neutral one, as in the case of the C(1) derivatives in the present work for the hydrogen bond to the His13 backbone NH, only marginally lowers the energy by 0.2 kcal/mol. Taking the amide derivative as an example, modeling suggests that three water-mediated hydrogen bonds are lost in addition to the altered hydrogen bond just mentioned. However, the bond to the Trp88 NH suffers from poor geometry and the loss of such a bond could actually improve binding (*46*). Making the conservative estimate that each of the two good hydrogen bonds are worth 1 kcal/mol, this would leave the altered hydrogen bond approximately energetically equivalent to the same bond in the native complex (see Table II) since, to a first approximation, entropic factors are the same for native GM1 and the derivative upon binding. Concerning the alcohol derivative, a slightly higher overall energetic cost is paid even though one hydrogen bond less is lost as compared to the amide derivative. However, a higher price has to be paid for the hydroxymethyl group (compared to the amide) to assume the conformation allowing this hydrogen bond.

For bulky derivatives, the situation is more complex as exemplified by the benzylamide derivative. Even though water molecules 2 and 3 are expelled there is no net loss of hydrogen bonds since they reform with bulk water. However, compared to CT-B binding of native GM1, where a net gain of hydrogen bonds occurs, there is a loss. In addition, the slight conformational change involving the sialic acid has to be considered. Opposing effects consist of a loss of unfavorable water interactions with the hydrophobic benzyl moiety in the free derivative and extensive van der Waals interactions between the toxin and the benzyl group. In total at least four hydrogen bonds, corresponding to 2-6 kcal/mol (*46*), are lost upon binding of the benzylamide derivative. By the same conservative estimate as above, the energy cost for the loss of these hydrogen bonds would be 4 kcal/mol, leaving approximately 1.4 kcal/mol to be contributed by the van der Waals interactions of the benzyl moiety. The cyclohexylmethylamide derivative displays an almost identical free energy difference as expected, whereas for butylamide, these contributions approximately cancel out the observed energy change (Table II), consistent with the substantially fewer van der Waals contacts observed between the butyl chain and the protein. Finally, for the C(7) derivatives, the three hydrogen bonds mediated by water molecules 2 and 3 are lost but opposing hydrophobic contributions render these derivatives almost as active as native GM1. This is in line with previous observations involving even larger substituents like Lucifer Yellow or rhodamine (*13*). There is also a good correlation between the extent of these hydrophobic interactions and the observed relative free energy changes.

Among the recently reported crystal structures of a number of different galactosyl derivatives in complex with heat-labile enterotoxin B-pentamers (LT-B) from porcine-derived *E. coli*, the LT-B-meta-nitrophenyl-D-galactoside complex (*40*) is found to be of relevance for the complex between CT-B and bulky C(1) derivatives, especially the cyclohexylmethylamide and benzylamine derivatives. Overlapping the latter structure with the LT-B complex reveals that the nitrophenyl moiety points in the same direction towards Gly33 as the benzylamide group but with the phenyl ring rotated approximately 65° relative to the benzyl ring. The benzyl ring plane is also more or less parallel to the Tyr12 ring plane in contrast to the phenyl ring. Another difference is that the Gln61 side chain has rotated 180° in the LT-B-meta-nitrophenyl-D-galactoside complex. However, given the different sites of attachment of these substituents, there is a remarkable topographical similarity of which the almost identical affinities relative to GM1 are proof.

Maria Svensson is gratefully acknowledged for analyses of CT-B binding to GM2 and Thomas Larsson for acquiring mass spectra.

REFERENCES

1. van Heyningen, W.E., Carpenter, C.C.J., Pierce, N.F., and Greenough III, W.B. (1971) Deactivation of cholera toxin by ganglioside. *J. Infect. Dis.* **124**, 415-418
2. Spangler, B.D. (1992) Structure and function of cholera toxin and the related *Escherichia coli* heat-labile enterotoxin. *Microbiol. Rev.* **56**, 622-647
3. Lundgren, O. and Jodal, M. (1997) The enteric nervous system and cholera toxin-induced secretion. *Comp. Biochem. Physiol.* **118A**, 319-327
4. Hakomori, S.-i. (1983) Chemistry of glycosphingolipids in *Sphingolipid Biochemistry* (Kanfer, J.N. and Hakomori, S.-i., eds.) Vol. 3, pp. 1-165, Plenum Press, New York
5. Solís, D., Jiménez-Barbero, J., Martín-Lomas, M., and Díaz-Maurino, T. (1994) Probing hydrogen-bonding interactions of bovine heart galectin-1 and methyl β-lactoside by use of engineered ligands. *Eur. J. Biochem.* **223**, 107-114
6. Vermersch, P.S., Tesmer, J.J.G., and Quiocho, F. (1992) Protein-ligand energetics assessed using deoxy and fluorodeoxy sugars in equilibrium binding and high resolution chrystallographic studies. *J. Mol. Biol.* **226**, 923-929
7. Ångström, J., Teneberg, S., and Karlsson, K.-A. (1994) Delineation and comparison of ganglioside binding epitopes for the toxins of *Vibrio cholerae, Escherichia coli* and *Clostridium tetani*: Evidence for overlapping epitopes. *Proc. Natl. Acad. Sci. USA* **91**, 11859-11863
8. Fishman, P.H., Pacuszka, T., Hom, B., and Moss, J. (1980) Modification of the ganglioside GM1. *J. Biol. Chem.* **255**, 7657-7664
9. Kazuya, I.-P., Hidari, K.I.-P.J., Irie, F., Suzuki, M., Kon, K., Ando, S., and Hirabayashi, Y. (1993) A novel ganglioside with a free amino group in bovine brain. *Biochem. J.* **296**, 259-263
10. Lanne, B., Schierbeck, B., and Karlsson, K.-A. (1994) On the role of the carboxyl group of sialic acid in binding of cholera toxin to the receptor glycosphingolipid, GM1. *J. Biochem.* **116**, 1269-1274
11. Masserini, M., Freire, E., Palestini, P., Calappi, E., and Tetta-

manti, G. (1992) Fuc-GM1 ganglioside mimics the receptor function of GM1 for cholera toxin. *Biochemistry* **31**, 2422-2426
12. Schengrund, C.-L. and Ringler, N.J. (1989) Binding of *Vibrio cholerae* toxin and the heat-labile enterotoxin of *Escherichia coli* to G_{M1}, derivatives of G_{M1}, and nonlipid oligosaccharide polyvalent ligands. *J. Biol. Chem.* **264**, 13233-13237
13. Spiegel, S. (1985) Fluorescent derivatives of ganglioside GM1 function as receptors for cholera toxin. *Biochemistry* **24**, 5947-5952
14. Moreno, E., Lanne, B., Vázquez, A.M., Kawashima, I., Tai, T., Fernández, L.E., Karlsson, K.-A., Ångström, J., and Pérez, R. (1998) Delineation of the epitope recognized by an antibody specific for *N*-glycolylneuraminic acid-containing gangliosides. *Glycobiology* **8**, 695-705
15. Merritt, E.A., Sarfaty, S., van den Akker, F., L'hoir, C., Martial, J.A., and Hol, W.G.J. (1994) Crystal structure of cholera toxin B-pentamer bound to receptor G_{M1} pentasaccharide. *Protein Sci.* **3**, 166-175
16. Zhang, R.-G., Scott, D.L., Westbrook, M.L., Nance, S., Spangler, B.D., Shipley, G.G., and Westbrook, E.M. (1995) The three-dimensional crystal structure of cholera toxin. *J. Mol. Biol.* **251**, 563-573
17. Hanisch, F.-G., Hacker, J., and Schroten, H. (1993) Specificity of S fimbriae on recombinant *Escherichia coli*: preferential binding to gangliosides expressing NeuGcα(2-3)Gal and NeuAcα(2-8) NeuAc. *Infect. Immun.* **61**, 2108-2115
18. Stults, C.L., Sweeley, C.C., and Macher, B.A. (1989) Glycosphingolipids: structure, biological source, and properties. *Methods Enzymol.* **17**, 167-214
19. Karlsson, K.-A. (1974) Carbohydrate composition and sequence analysis of a derivative of brain disialoganglioside by mass spectrometry, with molecular weight ions at *m/e* 2245. Potential use in the specific microanalysis of cell surface components. *Biochemistry* **13**, 3643-3647
20. Larson, G., Karlsson, H., Hansson, G.C., and Pimlott, W. (1987) Application of a simple methylation procedure for the analyses of glycosphingolipids. *Carbohydr. Res.* **161**, 281-290
21. Aggarwal, B.B., Eessalu, T.E., and Hass, P.E. (1985) Characterization of receptors for human tumour necrosis factor and their regulation by γ-interferon. *Nature* **318**, 665-667
22. Lanne, B., Uggla, L., Stenhagen, G., and Karlsson, K.-A. (1995) Enhanced binding of enterotoxigenic *Escherichia coli* K99 to amide derivatives of the receptor ganglioside NeuGc-GM3. *Biochemistry* **34**, 1845-1850
23. Veh, R.W., Cornfield, A.P., Sander, M., and Schauer, R. (1977) Neuraminic acid-specific modification and tritium labelling of gangliosides. *Biochim. Biophys. Acta* **486**, 145-160
24. Michalek, M.T., Mold, C., and Bremer, E.G. (1988) Inhibition of the alternative pathway of human complement by structural analogues of sialic acid. *J. Immunol.* **140**, 1588-1594
25. Dubois, M., Gilles, K.A., Hamilton, J.K., Rebers, P.A., and Smith, F. (1956) Colorimetric method for determination of sugars and related substances. *Anal. Chem.* **28**, 350-356
26. Svennerholm, L. (1963) Chromatographic separtion of human brain gangliosides. *J. Neurochem.* **10**, 613-623
27. Karlsson, K-A. and Strömberg, N. (1987) Overlay and solid-phase analysis of glycolipid receptors for bacteria and viruses. *Methods Enzymol.* **138**, 220-231
28. Ogura, K., Ogura, M., Anderson, R.L., and Sweeley, C.C. (1992) Peroxidase-amplified assay of sialidase activity toward gangliosides. *Anal. Biochem.* **200**, 52-57
29. Scopsi, L. and Larsson, L.-I. (1986) Increased sensitivity in peroxidase immunohistochemistry. *Histochemistry* **84**, 221-230
30. Mayo, S.L., Olafsen, B.D., and Goddard III, W.A. (1990) Dreiding: a generic force field for molecular simulations. *J. Chem. Phys.* **94**, 8897-8909
31. Rappé, A.K. and Goddard III, W.A. (1991) Charge equilibration for molecular dynamics simulations. *J. Chem. Phys.* **95**, 3358-3363
32. Karlsson, K.-A., Teneberg, S., Ångström, J., Kjellberg, A., Hirst, T.R., Bergström, J., and Miller-Podraza, H. (1996) Unexpected carbohydrate cross-binding by *Escherichia coli* heat-labile enterotoxin. Recognition of human and rabbit target cell glycoconjugates in comparison with cholera toxin. *Bioorg. Med. Chem.* **4**, 1919-1928
33. Ravindranath, M.H., Ravindranath, R.M.H., Morton, D.L., and Graves, M.C. (1994) Factors affecting the fine specificity and sensitivity of serum antiganglioside antibodies in ELISA. *J. Immunol. Methods* **169**, 257-272
34. Dressen, F., Uhlenbruck, G., and Hanish, F.-G. (1992) A quantitative microassay of carbohydrate-mediated cell adhesion to glycoconjugates immobilized on polystyrene plates. *Anal. Biochem.* **206**, 369-375
35. Lanne, B. (1997) A method to eliminate sucrose from gangliosides and other glycosphingolipids. *Anal. Biochem.* **252**, 205-207
36. Acquotti, D., Fronza, G., Riboni, L., Sonnino, S., and Tettamanti, G. (1987) Ganglioside lactones: ^{1}H-NMR determination of the inner ester position of GD1b-ganglioside lactone naturally occurring in human brain or produced by chemical synthesis. *Glycoconj. J.* **4**, 119-127
37. Sabesan, S., Bock, K., and Lemieux, R.U. (1984) The conformational properties of the gangliosides G_{M2} and G_{M1} based on ^{1}H and ^{13}C nuclear magnetic resonance studies. *Can. J. Chem.* **62**, 1034-1045
38. Levery, S.B. (1991) ^{1}H-NMR study of G_{M2} ganglioside: evidence that an interresidue amide-carboxyl hydrogen bond contributes to stabilization of a preferred conformation. *Glycoconj. J.* **8**, 484-492
39. Siebert, H.-C., Reuter, G., Schauer, R., von der Lieth, C.-W., and Dabrowski, J. (1992) Solution conformations of GM3 gangliosides containing different sialic acid residues as revealed by NOE-based distance mapping, molecular mechanics, and molecular dynamics simulations. *Biochemistry* **31**, 6962-6971
40. Merritt, E.A., Sarfaty, S., Feil, I.K., and Hol, W.G.J. (1997) Structural foundation for the design of receptor antagonists targeting *Escherichia coli* heat-labile enterotoxin. *Structure* **5**, 1485-1499
41. Cautrecasas, P. (1973) Interaction of *Vibrio cholerae* enterotoxin with cell membranes. *Biochemistry* **12**, 3547-3558
42. Fukuta, S., Magnani, J.L., Twiddy, E.M., Holmes, R.K., and Ginsburg, V. (1988) Comparison of the carbohydrate-binding specificities of cholera toxin and *Escherichia coli* heat-labile enterotoxins LTh-I, LT-IIa and LT-IIb. *Infect. Immun.* **56**, 1748-1753
43. Kuziemko, G.M., Stroh, M., and Stevens, R.C. (1996) Cholera toxin binding affinity and specificity for gangliosides determined by surface plasmon resonance. *Biochemistry* **35**, 6375-6384
44. MacKenzie, C.R., Hirama, T., Lee, K.K., Altman, E., and Young, N.M. (1997) Quantitative analysis of bacterial toxin affinity and specificity for glycolipid receptors by surface plasmon resonance. *J. Biol. Chem.* **272**, 5533-5538
45. Schön, A. and Freire, E. (1989) Thermodynamics of intersubunit interactions in cholera toxin upon binding to the oligosaccharide portion of its cell surface receptor, ganglioside G_{M1}. *Biochemistry* **28**, 5019-5024
46. Fersht, A.R., Shi, J.-P., Knill-Jones, J., Lowe, D.M., Wilkinson, A.J., Blow, D.M., Brick, P., Waye, M.M.Y., and Winter, G. (1985) Hydrogen bonding and biological specificity analysed by protein engineering. *Nature* **314**, 235-238